Psilocybin reduces functional connectivity and the encoding of spatial information by neurons in mouse retrosplenial cortex

Victorita E. Ivan[1]*, David P. Tomàs-Cuesta[1]*, Ingrid M. Esteves[1], Artur Luczak[1], Majid[1] Mohajerani[1,2], Bruce L. McNaughton[1,3], Aaron J. Gruber[1]✉

[1]Canadian Center for Behavioural Neuroscience, Department of Neuroscience, University of Lethbridge, Lethbridge, Alberta, Canada

[2]Douglas Research Centre, Department of Psychiatry, McGill University

[3]Center for the Neurobiology of Learning and Memory, University of California Irvine, Irvine, California, USA

*The authors contributed equally.

✉ Aaron J. Gruber

Email: aaron.gruber@uleth.ca

Keywords: retrosplenial cortex, psychedelics, ketanserin, mutual information, serotonin

Abstract

Psychedelic drugs have profound effects on perception, cognition, and mood. How psychedelics affect neural signaling to produce these effects remains poorly understood. We investigated the effect of the classic psychedelic psilocybin on neural activity patterns and spatial encoding in the retrosplenial cortex of head-fixed mice navigating on a treadmill. The place specificity of neurons to distinct locations along the belt was reduced by psilocybin. Moreover, the stability of place-related activity across trials decreased. Psilocybin also reduced the functional connectivity among simultaneously recorded neurons. The 5-HT_{2A}R (serotonin 2A receptor) antagonist ketanserin blocked the majority of these effects. These data are consistent with proposals that psychedelics increase the entropy of neural signaling, and provide a potential neural mechanism contributing to disorientation frequently reported by humans after taking psychedelics.

Introduction

Psychedelic drugs have profound acute effects on perception, cognition, and mood. Molecules affecting a variety of neurotransmitter receptor types have psychedelic properties. The serotonin, or hydroxytryptophan (5-HT), 2A receptor has been identified as the primary mediator of the psychedelic effects of classic psychedelics, such as psilocybin (Vollenweider et al., 1998; Quednow et al., 2012). 5-HT can modulate neural activity in the brain's neocortex through presynaptic and postsynaptic neuromodulatory effects on cortical neurons (Andrade, 2011), which express a variety of 5-HT receptor types. Several primary effects of psilocybin are blocked by the 5-HT_{2A} antagonist ketanserin (Kometer et al., 2012; Torrado Pacheco et al., 2023). Ketanserin, however, does not block all of its effects (Carter et al., 2005; Hesselgrave et al., 2021). Therefore, non-5-HT_{2A} receptors likely contribute to the effects of psilocybin on mentation.

The effects of psilocybin on neural encoding and brain dynamics have largely been studied using non-invasive imaging in humans (Carhart-Harris et al., 2012; Carhart-Harris et al., 2017b; Daws et al., 2022). This work suggests that the coordination of activity among brain regions becomes less structured (Muthukumaraswamy et al., 2013; Varley et al., 2020). It remains to be determined if this also occurs at the level of neurons, and if this is due more to corruption of the inputs to cortical networks involved in perception, or more due to corruption of the dynamics within these networks. The few existing studies of cellular-level effects in behaving animals report discrepant effects. A recent study of visual cortex showed little effect of a classic psychedelic (2,5-dimethoxy-4-iodoamphetamine; DOI) on responses to visual inputs in mouse primary visual cortex (Michaiel et al., 2019). On the other hand, we reported that the non-classic psychedelic ibogaine significantly degrades the encoding of spatial information in a cortical region called the retrosplenial cortex (RSC) (Ivan et al., 2023). The discrepancy between these studies may involve differences in brain

region and/or the pharmacology of the psychedelic used. Here, we test if the classic psychedelic psilocybin degrades spatial information similarly to ibogaine, and if this depends on 5-HT_{2A} receptors.

The RSC encodes the spatial state of animals within an environment and supports navigation in freely moving animals (Keene and Bucci, 2009; Alexander and Nitz, 2015). Some RSC neurons activate when an animal traverses specific regions of an environment, similar to 'place cells' in the hippocampus (O'Keefe and Nadel, 1978). RSC neurons generate similar place cells in head-fixed animals navigating virtual environments (Mao et al., 2017; Esteves et al., 2021). The RSC is a key node in a network linking the hippocampus (HPC) with the medial prefrontal cortex (mPFC) (Wyass and Van Groen, 1992; Fisk and Wyss, 1999; Shibata et al., 2004). This network is involved in generating representations of environments via cognitive maps (O'Keefe and Nadel, 1978; Iaria et al., 2007), and navigation decisions to achieve goals. 5-HT appears to affect this processing. Psilocin, psilocybin's active metabolite, causes a decrease in the BOLD signal relative to baseline in the cingulate and retrosplenial cortical regions of rats (Spain et al., 2015). Conversely, resting-state fMRI in anesthetized mice found an increase in functional connectivity (FC) between these two regions and other structures expressing the 5-HT_{2A} receptors, such as the ventral striatum (Grandjean et al., 2021). RSC interactions with other structures thus appears to be modulated by psychedelics. The spatial information encoded in this region provides a means to assess how these psychedelics affect neural information processing at the cellular level. Here, we quantify how psilocybin, with or without blockage of 5-HT_{2A} receptors, affect spatial representation and neural dynamics of large ensembles of neurons in RSC as head-fixed mice navigate a virtual environment.

Methods

Animals

Adult (4-9 month old) Thy1-GCaMP6m mice (n=10; 2F/8M), weighing 19-28 g, were housed in standard rodent cages, and maintained at 24 °C under a 12 h light/dark cycle. Mice had free access to food and water before training. All experiments were performed during the light cycle (between 7:30 AM and 7:30 PM). Procedures were in accordance with the guidelines established by the Canadian Council on Animal Care, and with protocols approved by the Animal Welfare Committee of the University of Lethbridge.

Surgery

Before surgery, animals received buprenorphine (0.05 mg/kg SC) and dexamethasone (0.2 mg/kg IM). They were then anesthetized with isoflurane (1-1.5%) and head fixed in a stereotaxic frame with body temperature maintained at 37.0 ± 0.5 ◦C with a heating pad. Mice received a 5 mm bilateral craniotomy (AP: +1 to -4; ML: -2.5 to +2.5), which was then covered with three layers of coverslips affixed with optical adhesive (NOA71, Norland). The coverslip was attached to the skull using Vetbond, and a titanium head plate was fixed to the skull using metabond. Post-surgical care included careful weight monitoring and subcutaneous injections of meloxicam (Metacam 1 mg/kg) and enrofloxacin (Baytril, 10 mg/kg) for three days after implant.

Drugs

Psilocybin was obtained from Toronto Research Chemicals, Canada, in powder form and diluted in sterile water in order to achieve a dose of 1.5 or 15 mg/kg in a 0.1 ml volume for each mouse.

Ketanserin tartrate salt was obtained from Sigma-Aldrich Canada, in powder form, and dissolved in 20% DMSO, and the stock solutions were stored at −20 °C. The stock solutions were prepared on the day of injection when possible and diluted in saline to achieve a dose of 1 or 5 mg/kg. The control animals received 0.1 ml 0.9% saline solution. All injections were intraperitoneal.

Experimental procedure for behaviour

Head-fixed mice were trained to run on a treadmill using a positive reinforcement paradigm. They received a drop of 10% sucrose solution on every trial, consisting of one lap of the treadmill belt. Animals were water restricted during the training and testing. They had ad libitum access to water for up to 30 minutes per day, and their body weight was carefully monitored throughout the experiment to ensure the weight loss did not exceed 15% of their baseline value. The treadmill belt consisted of a Velcro strip that was 150 cm long and 4 cm wide. Three tactile cues were placed in different locations on the belt. Additionally, we used one auditory cue (1kHz) and one blue light LED cue that each activated at a specific and constant belt position. An optical encoder attached to the wheel shaft was used to monitor belt movement. A microcontroller was used to monitor the encoder, licking sensor, and the reward delivery. Training continued in daily sessions until mice performed at least 20 trials in 20 minutes. Mice were trained on one belt and then transferred to a new belt for the imaging sessions.

Neural activity was imaged in daily sessions of the task for 15-20 minutes. For drug days, we recorded first a baseline activity (+/- saline/ketanserin) for 10 mins in every session, then mice (n = 7) were given an injection of psilocybin or saline and recorded again for 10 minutes. Recordings were performed starting at 10 minutes after each injection. Each animal was imaged for one session before any injections, for two days of saline injections, and then received 4 days of psilocybin

every other day, with or without the ketanserin pretreatment. The control group (n = 3) received only saline in the same schedule as the treatment group.

Two-Photon Imaging

Neural activity was imaged using a 2-photon microscope (Bergamo II multiphoton microscopy, Thorlabs) through a 16x water-immersion objective lens (NA=0.8, Nikon). Excitation was with a Ti:sapphire pulsed laser (Coherent) tuned to a wavelength of 920 nm, ~80mW power, and controlled by a galvo-resonant X-Y scanner. Images were acquired at depths between 135 μm – 160 μm (layer II/III), from a field of view of 835 x 835 μm. Images were digitized at a sampling rate of 19 Hz, and at a resolution of 800 x 800 pixels. Imaging data from all animals were acquired from one hemisphere of either the left or right RSC (AP: -1 to -3 mm; ML: 0 to +/- 1 mm).

Pre-processing

Automatic image pre-processing was performed using the Suite-2P algorithm (Pachitariu et al., 2017), as previously described (Mao et al., 2017; Mao et al., 2018). The regions of interest (ROIs) detected were inspected manually and labelled as cells or non-cells by experienced users. For each ROI, the ΔF/F time courses were deconvolved using constrained non-negative matrix factorization (Pnevmatikakis et al., 2016), and all subsequent analyses were conducted using the deconvolved time-courses. For injection days, the imaging sequences of both pre- and post-injection intervals were combined during pre-processing so as to acquire the activity of the same set of cells (ROIs) before and after injections.

Computing spatial encoding

In order to identify spatially tuned neurons, we computed the adjusted mutual information (MI) (Vinh et al., 2010) between the firing rate of each neuron and the position of the mouse in the belt. We first divided the belt into 50 bins (3 cm each). For each bin and trial, we summed the neuron's activity and binned it into 4 levels, giving us the joint bin-activity discrete distribution, which we use to compute the mutual information. The MI used here is an adjustment of mutual information which accounts for the number of trials, which differs number among session, and thus is appropriate to compare cells from different sessions on the same scale. The MI is upperlimited by 1 and takes an expected value of 0 when the firing and position are independent. Negative values signify that the MI for that cell is lower than the MI one would expect solely due chance.

Unit functional connectivity

Computing the apparent functional connectivity among neurons involved several steps. First, the spikes underlying the calcium fluorescence traces were inferred using a deconvolution algorithm (Friedrich et al., 2017). Next, the data in which the mouse is slow or not moving (below the 10% quantile of the velocity distribution over the track) is removed. The track is then divided into 50 spatial bins. The trial-averaged activity in each bin is computed for each cell to create a 'tuning curve' over the belt. The Pearson correlation between the tuning curves of all cell pairs is then computed. To visualize clusters in the cells x cells spatial correlation matrix, the columns/rows were ordered so that highly correlated cells are adjacent. For each neuron, a vector of its correlations with all other cells was generated. In order to determine the similarity between the correlation structures, the pairwise euclidean distances between those vectors were calculated. Using the unweighted pair group method with arithmetic mean (UPGMA), a hierarchical clustering on these measures was conducted (Sokal, 1958). To assess the amount of

clustering in the spatial correlation matrices, we computed the average clustering coefficient (Saramäki et al., 2007), a measure which quantifies how many cells with similar firing patterns are similar between each other, averaged over all cells; this coefficient is independent of the ordering of rows/columns.

Results

We used 2-photon imaging to record the activity of ensembles of individual neurons (112-732 simultaneous cells per session; mean = 380.6, STD = 100.1) in the superficial layers (135 – 160 μm; layer II/III) of RSC in head-fixed mice (Fig. 1.A). Mice were recorded while running on a treadmill belt that had narrow tactile cues laid across the width of the belt in three positions along its length, as well as one auditory cue and one light cue that each activated at specific places in the virtual environment (i.e. belt position). After running for one full lap of the belt, the animals received a 10% sucrose reward. Mice were injected (i.p.) with saline 10 mins prior to task initiation and neural recordings were performed for a 10-minute baseline ("before") period. They were then injected with either psilocybin (15 mg/kg) or the same volume of saline vehicle 10 mins prior to a second neural recording period. We used both within-session (recording before & after 2nd injection) and within-animal (each received psilocybin or saline on different sessions) controls. Statistical inference of drug effect was determined by 2-way (before/after injection x psilocybin/saline) repeated measures (RM) ANOVA.

Psilocybin injection lowered the animals' movement velocity (Fig. 1.B; RM two-way ANOVA; $F(3, 18) = 9.962$, $p < 0.001$; Sidak's post-hoc for psilocybin $p = 0.001$), and reduced the number of trials per minute completed (Fig. 1.C; Mixed-effects model; $F(3, 18) = 13.12$, $p < 0.0001$; Sidak's

post-hoc p = 0.002). Psilocybin did not affect the proportion of time the animals were stationary between the start of a lap and the arrival at the feeder location (stop ratio; Fig. 1.D; RM two-way ANOVA; F (3, 18) = 5.609, p = 0.007; Sidak's post-hoc for psilocybin p = 0.636). The psilocybin-induced retardation of locomotion is consistent with previous reports (Halberstadt et al., 2011; Tylš et al., 2016). The average neural activity rate also decreased after drug administration (Fig. 1.E; two-way ANOVA; F (3, 18) = 7.532, p = 0.002; Sidak's post-hoc p = 0.045). A second cohort of animals that only ever received saline showed no significant effect of injection on any of these measures (Supplemental Fig. 1).

Many RSC neurons have place-specific activity, activating at specific locations on the belt during each trial (Fig. 2.A), whereas other cells are not selective to particular positions or have high variability. In order to quantify the amount of spatial information conveyed by each neuron, we computed an adjusted form of mutual information (MI) between each cell's activity and belt position (details in methods). This metric captures variance of activity along one lap of the belt, as well as variance from trial to trial (Souza et al., 2018). We then restricted analysis of spatial encoding to the cells that were most selective to position (top quartile of MI distribution). Psilocybin significantly decreased the mean MI of these cells (Fig. 2.B; REML: F (1, 23) = 6.406, p = 0.019; ROUT (Q = 1%; n=1)). We also investigated the average cross correlation of position-dependent cellular activity between trials to assess the stability of spatial tuning. These trial-to-trial correlations decreased after psilocybin but not saline (Fig. 2.C; REML: F (1, 23) = 19.51, p = 0.0002; ROUT (Q = 1%; n=1)), suggesting less stability of spatial representations after administration of psilocybin as compared to saline.

We next sought to determine if psilocybin affected the functional connectivity among cells within the RSC. We computed the pair-wise correlation of activity among all neurons recorded

simultaneously during a session, and used hierarchical clustering to order the units so that functionally similar units were adjacent. We applied the same matrix ordering to the activity of the same cells collected after psilocybin administration to visualize any changes in correlation structure (Fig. 2.D). We quantified psychedelic-induced changes in functional connectivity patterns by computing the clustering coefficient of the correlation matrix. This quantifies the statistics of functionally-similar units. It is high when there are multiple clusters, each of which containing functionally-similar units. Psilocybin reduced the clustering coefficient (Fig. 2.E; RM two-way ANOVA; $F(1, 6) = 14.01$, $p = 0.009$), indicating a loss of functional connectivity structure. In other words, each neuron is activating more independently from the others.

We next investigated if these effects of psilocybin on neural activity were mediated by 5-HT_{2A}R by injecting ketanserin (an antagonist of this receptor) prior to the baseline recording period, and then injecting psilocybin prior to the second recording period. We used a randomized schedule of injection after baseline recordings. Treatments were: low dose ketanserin (k; 1 mg/kg) followed by low dose psilocybin (p; 1.5 mg/kg; n = 3); low dose ketanserin followed by high dose psilocybin (**P**; 15 mg/kg; n = 4); or high dose ketanserin (**K**; 5 mg/kg) followed by high dose psilocybin (n = 3). Low dose ketanserin blocked the effects of high or low dose psilocybin on behaviour, firing rate, MI, trial-to-trial correlation, and clustering of cross-correlations (Fig. 3. C-D; Supplemental Fig. 2; Supplemental Table 1). The high dose ketanserin did not fully block the effects of high psilocybin on MI (Fig. 3.A; RM two-way ANOVA; $F(3, 6) = 13.53$, $p = 0.004$; Sidak's post-hoc $p = 0.046$) or firing rate (Fig. 3.B; RM two-way ANOVA; $F(3, 6) = 10.40$, $p = 0.009$; Sidak's post-hoc $p = 0.013$). Nonetheless, it appears that ketanserin blocks or reduces the effects of psilocybin on both behaviour and neural activity, suggesting that 5-HT_{2A}R are involved in the phenomena.

Discussion

In this study, psilocybin reduced locomotion, decreased spatial information encoded by RSC cells, and decreased functional connectivity among RSC neurons. The 5-HT_{2A} antagonist ketanserin blocked the behavioural effects and prevented the loss of spatial information at a dose of 1 mg/kg. Unexpectedly, the higher dose of ketanserin (5 mg/kg) did not fully block effects of psilocybin on firing rate and MI. Nonetheless, the preponderance of evidence suggests that the effects of psilocybin in this study are primarily mediated by 5-HT_{2A}R.

The administration of psilocybin reduced locomotion speed in the present data, similar to previous reports (Halberstadt et al., 2011; Tylš et al., 2016). Psilocybin also decreased the mean activity rate of RSC neurons in this study, which contrasts the increase in RSC activity rate by the non-classic psychedelic ibogaine in our previous study using the same experimental apparatus (Ivan et al., 2023). We are unaware of other prior studies examining effects of psychedelics on RSC neuron activity, but there are some limited data in functionally related brain structures. Lower doses of psilocybin (2 mg/kg) increased the firing rate of ACC neurons in head-fixed mice running on a treadmill (Golden and Chadderton, 2022). Similarly, 5-MeO-DMT also increased activity rates in a majority of neurons recorded in layer V of ACC in anesthetized rats (Riga et al., 2014). This psychedelic and psilocybin increase excitatory post-synaptic currents of pyramidal neurons in brain slices of prefrontal cortex (Shao et al., 2021; Vargas et al., 2023). In contrast, a psilocybin-containing extract decreased neuronal spiking in the majority of CA1 pyramidal neurons in brain-slices of HPC (Moldavan et al., 2000). It is unclear if these discrepant effects of psychedelics on firing rate is due to dose, brain structure, locomotion, or other factors.

Psilocybin caused a large-scale reorganization of the relationship of activity among RSC neurons. After psilocybin administration, the dominant motifs of pair-wise correlation structure are

dispersed, indicating that the most common patterns of RSC activity during baseline largely vanish. This pattern is consistent across sessions and animals, indicating that acute psilocybin causes a restructuring of functional connectivity (FC) among neurons. This effect can be partially explained by the destabilization of positional signaling. In human fMRI studies, psychedelic drugs have been generally reported to increase the distribution of activity covariance motifs among brain regions (Tagliazucchi et al., 2014; Atasoy et al., 2017), and promote cortical desynchronization (Muthukumaraswamy et al., 2013; Riga et al., 2018). Psilocybin has been shown to particularly affect the FC within the default-mode network (DMN), which includes RSC (Carhart-Harris et al., 2012; Roseman et al., 2014; Daws et al., 2022). This effect of psilocybin to reduce FC in the DMN has also been reported in fMRI studies of rodents (Grandjean et al., 2021). The psychedelic-associated loss of functional connectivity is often associated with ego-dissolution, which was shown to correlate with decreased FC between the parahippocampal and retrosplenial cortex (Carhart-Harris et al., 2016; Lebedev et al., 2016). Both psilocybin and LSD significantly increase the 'complexity' of functional connectivity networks in the neocortex (Varley et al., 2020; Girn et al., 2022). Our results are consistent with these reports, and demonstrate similar dynamical changes at the cellular level within the RSC.

Acute psilocybin administration decreased the stability of RSC neuron encoding of position, shown by the reduced mutual information and trial-to-trial correlation of individual neurons. Many RSC cells encoded specific locations on the belt before psychedelic administration, as shown previously (Mao et al., 2017), but these cells are destabilized by psilocybin, similar to the effect of the non-classic psychedelic ibogaine (Ivan et al., 2023). However, despite the high dosage of psilocybin used here, the changes in spatial encoding were surprisingly weak as compared to those evoked by a moderate dose of ibogaine (Ivan et al., 2023). Multiple regions in the neocortex encode

position, environmental cues, and spatial information (Mashhoori et al., 2018; Esteves et al., 2021), which can provide a framework for navigation and context-dependent learning (Gruber and McDonald, 2012; Chang et al., 2020). Reports of human perceptual experience is consistent with psychedelic-based disruption of this information. Psychedelics often disrupt the sense of space and time, causing disorientation and a feeling of spacelessness (Carbonaro et al., 2016; Garcia-Romeu et al., 2016; Smigielski et al., 2019). It is unclear if the altered encoding of space in RSC is more due to the direct action of psilocybin in RSC, or to alterations of afferent information. RSC positional information relies on hippocampal processing (Esteves et al., 2021) in order to form and maintain the cognitive map (McNaughton et al., 2006). Psilocybin not only affects 5-HT receptors, but also alters glutamate levels in both the mPFC and the HPC (Mason et al., 2020). Interestingly, higher glutamate in mPFC correlated with negative experiences, whereas lower glutamate in HPC was associated with a pleasant state of ego dissolution. Rodent studies have likewise found that psilocybin or its active form psilocin can affect dopamine, serotonin, glutamate, and GABA levels in the frontal cortex and/or striatum (Sakashita et al., 2015; Wojtas et al., 2022) . These data suggest that the effect of psilocybin on RSC activity could involve modulation of several neurotransmitter systems in RSC and afferent structures.

Despite affecting several neurotransmitter systems, psilocybin exerts its psychoactive effects primarily through the 5-HT_{2A} receptor. The occupancy of these receptors in the neocortex relates closely to the intensity of the psychedelic effect (Madsen et al., 2019; Kringelbach et al., 2020). We found that blocking these receptors with ketanserin reduced the majority of the behavioural and neural activity effects caused by psilocybin. Interestingly, the low dose fully blocked effects, whereas the high dose did not. Prior rodent work has similarly shown only partial blockade of psilocybin effects at behavioural and synaptic levels with ketensarin or closely related molecules

(Moldavan et al., 2000; Hesselgrave et al., 2021; Torrado Pacheco et al., 2023). Indeed, other 5-HT receptors are involved in modulating behaviour. For instance, 5-HT_{1A} and 5-HT_{2C} receptors also contribute significantly the suppressing effect of psilocin on locomotion and investigatory behaviour in rats (Tylš et al., 2016) and mice (Halberstadt et al., 2011). Moreover, the effects of 5-HT blockade depend on cellular physiology and/or phenotype. For instance, systemic administration of ketanserin reduced conditioned freezing in rats bred to display enhanced freezing, but exerted the opposite effect in low-freezing animals (León et al., 2017). Besides the possible involvement of multiple 5-HT receptor subtypes, it is also possible that the pharmacodynamics contributed to the inability of ketanserin to fully block effects of psilocybin on spatial encoding in the present data, as psilocybin was administered 30 min after the antagonist. In previous reports, ketanserin pretreatment only partially reduced psilocybin-induced head-twitch behaviour when administered 1h before the psychedelic (Hesselgrave et al., 2021), but abolished it when administered 10 minutes before psilocybin (Shao et al., 2021). In sum, our data are consistent with prior studies in that they suggest some involvement of 5-HT_{2A} receptors in the effects of psilocybin, but do not rule out contributions of other neurotransmitter systems.

Conclusion

Although several fMRI studies in humans and rodents have indicated that psychedelics alter mesoscale brain activity levels and cross-regional coordination, little is known about how these drugs affect information representation and processing at the cellular level. The present data suggest that activity of individual RSC neurons become discoordinated from one another, and overall activity rates are reduced. These data are consistent with mesoscale effects reported in fMRI studies. Despite the discoordination among neurons, the representation of spatial position by individual neurons was only mildly impaired. This was surprising because of the high dose of

311 psilocybin administered (15 mg/kg), which in humans would evoke profound changes in
312 mentation. We therefore speculate that either the drug's effect on mentation is less intense in these
313 mice than is typical in humans, or that psychedelics effects are manifested by subtle changes to
314 neural encoding that are difficult to identify in the present experimental design.

315

316 **Acknowledgments**

317 We would like to thank Adam Neumann for technical support and Dr. HaoRan Chang for helpful
318 discussions. Funding provided by: Natural Sciences and Engineering Council of Canada, New
319 Frontiers Research Fund, Alberta Innovates, Beswick Fellowship, Canadian Institute of Health
320 Research.

321 Author Contributions: V.E.I. and A.J.G. designed research, V.E.I. and I.M.E. performed research,
322 M.M. contributed tools, V.E.I., D.P.T-C, and I.M.E. analyzed data, V.E.I., D.P.T-C, A.L., B.L.M.,
323 and A.J.G. wrote the paper.

324 Competing Interest Statement: The authors declare no competing interests.

325

326

327

328

329

330

References

Alexander, A.S., and Nitz, D.A. (2015). Retrosplenial cortex maps the conjunction of internal and external spaces. *Nature Neuroscience* 18(8), 1143-1151. doi: 10.1038/nn.4058.

Andrade, R. (2011). Serotonergic regulation of neuronal excitability in the prefrontal cortex. *Neuropharmacology* 61(3), 382-386. doi: https://doi.org/10.1016/j.neuropharm.2011.01.015.

Atasoy, S., Roseman, L., Kaelen, M., Kringelbach, M.L., Deco, G., and Carhart-Harris, R.L. (2017). Connectome-harmonic decomposition of human brain activity reveals dynamical repertoire re-organization under LSD. *Scientific Reports* 7(1), 17661. doi: 10.1038/s41598-017-17546-0.

Carbonaro, T.M., Bradstreet, M.P., Barrett, F.S., MacLean, K.A., Jesse, R., Johnson, M.W., et al. (2016). Survey study of challenging experiences after ingesting psilocybin mushrooms: Acute and enduring positive and negative consequences. *Journal of Psychopharmacology* 30(12), 1268-1278. doi: 10.1177/0269881116662634.

Carhart-Harris, R.L., Erritzoe, D., Williams, T., Stone, J.M., Reed, L.J., Colasanti, A., et al. (2012). Neural correlates of the psychedelic state as determined by fMRI studies with psilocybin. *Proceedings of the National Academy of Sciences* 109(6), 2138-2143. doi: 10.1073/pnas.1119598109.

Carhart-Harris, R.L., Muthukumaraswamy, S., Roseman, L., Kaelen, M., Droog, W., Murphy, K., et al. (2016). Neural correlates of the LSD experience revealed by multimodal neuroimaging. *Proceedings of the National Academy of Sciences* 113(17), 4853-4858. doi: 10.1073/pnas.1518377113.

Carhart-Harris, R.L., Roseman, L., Bolstridge, M., Demetriou, L., Pannekoek, J.N., Wall, M.B., et al. (2017b). Psilocybin for treatment-resistant depression: fMRI-measured brain mechanisms. *Scientific reports* 7(1), 1-11.

Carter, O.L., Burr, D.C., Pettigrew, J.D., Wallis, G.M., Hasler, F., and Vollenweider, F.X. (2005). Using psilocybin to investigate the relationship between attention, working memory, and the serotonin 1A and 2A receptors. *Journal of Cognitive neuroscience* 17(10), 1497-1508.

Chang, H., Esteves, I.M., Neumann, A.R., Sun, J., Mohajerani, M.H., and McNaughton, B.L. (2020). Coordinated activities of retrosplenial ensembles during resting-state encode spatial landmarks. *Philosophical Transactions of the Royal Society B: Biological Sciences* 375(1799), 20190228. doi: doi:10.1098/rstb.2019.0228.

Daws, R.E., Timmermann, C., Giribaldi, B., Sexton, J.D., Wall, M.B., Erritzoe, D., et al. (2022). Increased global integration in the brain after psilocybin therapy for depression. *Nature Medicine* 28(4), 844-851. doi: 10.1038/s41591-022-01744-z.

Esteves, I.M., Chang, H., Neumann, A.R., Sun, J., Mohajerani, M.H., and McNaughton, B.L. (2021). Spatial Information Encoding across Multiple Neocortical Regions Depends on an Intact Hippocampus. *The Journal of Neuroscience* 41(2), 307. doi: 10.1523/JNEUROSCI.1788-20.2020.

Fisk, G.D., and Wyss, J.M. (1999). Associational projections of the anterior midline cortex in the rat: intracingulate and retrosplenial connections. *Brain Research* 825(1), 1-13. doi: https://doi.org/10.1016/S0006-8993(99)01182-8.

Friedrich, J., Zhou, P., and Paninski, L. (2017). Fast online deconvolution of calcium imaging data. *PLOS Computational Biology* 13(3), e1005423. doi: 10.1371/journal.pcbi.1005423.

Garcia-Romeu, A., Kersgaard, B., and Addy, P.H. (2016). Clinical applications of hallucinogens: A review. *Experimental and clinical psychopharmacology* 24(4), 229-268. doi: 10.1037/pha0000084.

Girn, M., Roseman, L., Bernhardt, B., Smallwood, J., Carhart-Harris, R., and Nathan Spreng, R. (2022). Serotonergic psychedelic drugs LSD and psilocybin reduce the hierarchical differentiation of unimodal and transmodal cortex. *NeuroImage* 256, 119220. doi: https://doi.org/10.1016/j.neuroimage.2022.119220.

Golden, C.T., and Chadderton, P. (2022). Psilocybin reduces low frequency oscillatory power and neuronal phase-locking in the anterior cingulate cortex of awake rodents. *Scientific Reports* 12(1)**,** 12702. doi: 10.1038/s41598-022-16325-w.

Grandjean, J., Buehlmann, D., Buerge, M., Sigrist, H., Seifritz, E., Vollenweider, F.X., et al. (2021). Psilocybin exerts distinct effects on resting state networks associated with serotonin and dopamine in mice. *NeuroImage* 225**,** 117456. doi: https://doi.org/10.1016/j.neuroimage.2020.117456.

Gruber, A.J., and McDonald, R.J. (2012). Context, emotion, and the strategic pursuit of goals: interactions among multiple brain systems controlling motivated behavior. *Front Behav Neurosci* 6(50)**,** 50. doi: 10.3389/fnbeh.2012.00050.

Halberstadt, A.L., Koedood, L., Powell, S.B., and Geyer, M.A. (2011). Differential contributions of serotonin receptors to the behavioral effects of indoleamine hallucinogens in mice. *Journal of psychopharmacology* 25(11)**,** 1548-1561.

Hesselgrave, N., Troppoli, T.A., Wulff, A.B., Cole, A.B., and Thompson, S.M. (2021). Harnessing psilocybin: antidepressant-like behavioral and synaptic actions of psilocybin are independent of 5-HT2R activation in mice. *Proceedings of the National Academy of Sciences* 118(17)**,** e2022489118. doi: 10.1073/pnas.2022489118.

Iaria, G., Chen, J.-K., Guariglia, C., Ptito, A., and Petrides, M. (2007). Retrosplenial and hippocampal brain regions in human navigation: complementary functional contributions to the formation and use of cognitive maps. *European Journal of Neuroscience* 25(3)**,** 890-899. doi: https://doi.org/10.1111/j.1460-9568.2007.05371.x.

Ivan, V.E., Tomàs-Cuesta, D.P., Esteves, I.M., Curic, D., Mohajerani, M., McNaughton, B.L., et al. (2023). The non-classic psychedelic ibogaine disrupts cognitive maps. *Biological Psychiatry Global Open Science*. doi: https://doi.org/10.1016/j.bpsgos.2023.07.008.

Keene, C.S., and Bucci, D.J. (2009). Damage to the retrosplenial cortex produces specific impairments in spatial working memory. *Neurobiology of Learning and Memory* 91(4)**,** 408-414. doi: https://doi.org/10.1016/j.nlm.2008.10.009.

Kometer, M., Schmidt, A., Bachmann, R., Studerus, E., Seifritz, E., and Vollenweider, F.X. (2012). Psilocybin Biases Facial Recognition, Goal-Directed Behavior, and Mood State Toward Positive Relative to Negative Emotions Through Different Serotonergic Subreceptors. *Biological Psychiatry* 72(11)**,** 898-906. doi: https://doi.org/10.1016/j.biopsych.2012.04.005.

Kringelbach, M.L., Cruzat, J., Cabral, J., Knudsen, G.M., Carhart-Harris, R., Whybrow, P.C., et al. (2020). Dynamic coupling of whole-brain neuronal and neurotransmitter systems. *Proceedings of the National Academy of Sciences* 117(17)**,** 9566-9576. doi: 10.1073/pnas.1921475117.

Lebedev, A.V., Kaelen, M., Lövdén, M., Nilsson, J., Feilding, A., Nutt, D.J., et al. (2016). LSD-induced entropic brain activity predicts subsequent personality change. *Human Brain Mapping* 37(9)**,** 3203-3213. doi: https://doi.org/10.1002/hbm.23234.

León, L.A., Castro-Gomes, V., Zárate-Guerrero, S., Corredor, K., Mello Cruz, A.P., Brandão, M.L., et al. (2017). Behavioral Effects of Systemic, Infralimbic and Prelimbic Injections of a Serotonin 5-HT2A Antagonist in Carioca High- and Low-Conditioned Freezing Rats. *Frontiers in Behavioral Neuroscience* 11. doi: 10.3389/fnbeh.2017.00117.

Madsen, M.K., Fisher, P.M., Burmester, D., Dyssegaard, A., Stenbæk, D.S., Kristiansen, S., et al. (2019). Psychedelic effects of psilocybin correlate with serotonin 2A receptor occupancy and plasma psilocin levels. *Neuropsychopharmacology* 44(7)**,** 1328-1334. doi: 10.1038/s41386-019-0324-9.

Mao, D., Kandler, S., McNaughton, B.L., and Bonin, V. (2017). Sparse orthogonal population representation of spatial context in the retrosplenial cortex. *Nature Communications* 8(1)**,** 243. doi: 10.1038/s41467-017-00180-9.

Mao, D., Neumann, A.R., Sun, J., Bonin, V., Mohajerani, M.H., and McNaughton, B.L. (2018). Hippocampus-dependent emergence of spatial sequence coding in retrosplenial cortex. *Proceedings of the National Academy of Sciences* 115(31)**,** 8015. doi: 10.1073/pnas.1803224115.

Mashhoori, A., Hashemnia, S., McNaughton, B.L., Euston, D.R., and Gruber, A.J. (2018). Rat anterior cingulate cortex recalls features of remote reward locations after disfavoured reinforcements. *eLife* 7**,** e29793. doi: 10.7554/eLife.29793.

Mason, N.L., Kuypers, K.P.C., Müller, F., Reckweg, J., Tse, D.H.Y., Toennes, S.W., et al. (2020). Me, myself, bye: regional alterations in glutamate and the experience of ego dissolution with psilocybin. *Neuropsychopharmacology* 45(12)**,** 2003-2011. doi: 10.1038/s41386-020-0718-8.

McNaughton, B.L., Battaglia, F.P., Jensen, O., Moser, E.I., and Moser, M.-B. (2006). Path integration and the neural basis of the 'cognitive map'. *Nature Reviews Neuroscience* 7(8)**,** 663-678. doi: 10.1038/nrn1932.

Michaiel, A.M., Parker, P.R.L., and Niell, C.M. (2019). A Hallucinogenic Serotonin-2A Receptor Agonist Reduces Visual Response Gain and Alters Temporal Dynamics in Mouse V1. *Cell Reports* 26(13)**,** 3475-3483.e3474. doi: https://doi.org/10.1016/j.celrep.2019.02.104.

Moldavan, M., Solomko, E.F., Grodzinskaya, A.A., Storozhuk, V.M., and Lomberg, M.L. (2000). Neurotropic Effect of Extracts from the Hallucinogenic Mushroom Psilocybe cubensis (Earle) Sing.(Agaricomycetideae). In Vitro Studies. *International Journal of Medicinal Mushrooms* 2(4).

Muthukumaraswamy, S.D., Carhart-Harris, R.L., Moran, R.J., Brookes, M.J., Williams, T.M., Errtizoe, D., et al. (2013). Broadband Cortical Desynchronization Underlies the Human Psychedelic State. *The Journal of Neuroscience* 33(38)**,** 15171-15183. doi: 10.1523/jneurosci.2063-13.2013.

O'Keefe, J., and Nadel, L. (1978). *The Hippocampus as a Cognitive Map.* Oxford: Clarendon Press.

Pachitariu, M., Stringer, C., Dipoppa, M., Schröder, S., Rossi, L.F., Dalgleish, H., et al. (2017). Suite2p: beyond 10,000 neurons with standard two-photon microscopy. *Biorxiv*.

Pnevmatikakis, Eftychios A., Soudry, D., Gao, Y., Machado, T.A., Merel, J., Pfau, D., et al. (2016). Simultaneous Denoising, Deconvolution, and Demixing of Calcium Imaging Data. *Neuron* 89(2)**,** 285-299. doi: https://doi.org/10.1016/j.neuron.2015.11.037.

Quednow, B.B., Kometer, M., Geyer, M.A., and Vollenweider, F.X. (2012). Psilocybin-Induced Deficits in Automatic and Controlled Inhibition are Attenuated by Ketanserin in Healthy Human Volunteers. *Neuropsychopharmacology* 37(3)**,** 630-640. doi: 10.1038/npp.2011.228.

Riga, M.S., Lladó-Pelfort, L., Artigas, F., and Celada, P. (2018). The serotonin hallucinogen 5-MeO-DMT alters cortico-thalamic activity in freely moving mice: Regionally-selective involvement of 5-HT1A and 5-HT2A receptors. *Neuropharmacology* 142**,** 219-230. doi: https://doi.org/10.1016/j.neuropharm.2017.11.049.

Riga, M.S., Soria, G., Tudela, R., Artigas, F., and Celada, P. (2014). The natural hallucinogen 5-MeO-DMT, component of Ayahuasca, disrupts cortical function in rats: reversal by antipsychotic drugs. *International Journal of Neuropsychopharmacology* 17(8)**,** 1269-1282. doi: 10.1017/S1461145714000261.

Roseman, L., Leech, R., Feilding, A., Nutt, D.J., and Carhart-Harris, R.L. (2014). The effects of psilocybin and MDMA on between-network resting state functional connectivity in healthy volunteers. *Frontiers in Human Neuroscience* 8. doi: 10.3389/fnhum.2014.00204.

Sakashita, Y., Abe, K., Katagiri, N., Kambe, T., Saitoh, T., Utsunomiya, I., et al. (2015). Effect of psilocin on extracellular dopamine and serotonin levels in the mesoaccumbens and mesocortical pathway in awake rats. *Biological and Pharmaceutical Bulletin* 38(1)**,** 134-138.

Saramäki, J., Kivelä, M., Onnela, J.-P., Kaski, K., and Kertész, J. (2007). Generalizations of the clustering coefficient to weighted complex networks. *Physical Review E* 75(2)**,** 027105. doi: 10.1103/PhysRevE.75.027105.

Shao, L.-X., Liao, C., Gregg, I., Davoudian, P.A., Savalia, N.K., Delagarza, K., et al. (2021). Psilocybin induces rapid and persistent growth of dendritic spines in frontal cortex in vivo. *Neuron* 109(16)**,** 2535-2544.e2534. doi: https://doi.org/10.1016/j.neuron.2021.06.008.

Shibata, H., Kondo, S., and Naito, J. (2004). Organization of retrosplenial cortical projections to the anterior cingulate, motor, and prefrontal cortices in the rat. *Neuroscience Research* 49(1)**,** 1-11. doi: https://doi.org/10.1016/j.neures.2004.01.005.

Smigielski, L., Kometer, M., Scheidegger, M., Krähenmann, R., Huber, T., and Vollenweider, F.X. (2019). Characterization and prediction of acute and sustained response to psychedelic psilocybin in a mindfulness group retreat. *Scientific Reports* 9(1)**,** 14914. doi: 10.1038/s41598-019-50612-3.

Sokal, R.R. (1958). A statistical method for evaluating systematic relationships. *Univ. Kansas, Sci. Bull.* 38**,** 1409-1438.

Souza, B.C., Pavão, R., Belchior, H., and Tort, A.B.L. (2018). On Information Metrics for Spatial Coding. *Neuroscience* 375**,** 62-73. doi: https://doi.org/10.1016/j.neuroscience.2018.01.066.

Spain, A., Howarth, C., Khrapitchev, A.A., Sharp, T., Sibson, N.R., and Martin, C. (2015). Neurovascular and neuroimaging effects of the hallucinogenic serotonin receptor agonist psilocin in the rat brain. *Neuropharmacology* 99**,** 210-220. doi: https://doi.org/10.1016/j.neuropharm.2015.07.018.

Tagliazucchi, E., Carhart-Harris, R., Leech, R., Nutt, D., and Chialvo, D.R. (2014). Enhanced repertoire of brain dynamical states during the psychedelic experience. *Human Brain Mapping* 35(11)**,** 5442-5456. doi: 10.1002/hbm.22562.

Torrado Pacheco, A., Olson, R.J., Garza, G., and Moghaddam, B. (2023). Acute psilocybin enhances cognitive flexibility in rats. *Neuropsychopharmacology : official publication of the American College of Neuropsychopharmacology*. doi: 10.1038/s41386-023-01545-z.

Tylš, F., Páleníček, T., Kadeřábek, L., Lipski, M., Kubešová, A., and Horáček, J. (2016). Sex differences and serotonergic mechanisms in the behavioural effects of psilocin. *Behavioural Pharmacology* 27(4)**,** 309-320.

Vargas, M.V., Dunlap, L.E., Dong, C., Carter, S.J., Tombari, R.J., Jami, S.A., et al. (2023). Psychedelics promote neuroplasticity through the activation of intracellular 5-HT2A receptors. *Science* 379(6633)**,** 700-706. doi: doi:10.1126/science.adf0435.

Varley, T.F., Carhart-Harris, R., Roseman, L., Menon, D.K., and Stamatakis, E.A. (2020). Serotonergic psychedelics LSD & psilocybin increase the fractal dimension of cortical brain activity in spatial and temporal domains. *NeuroImage* 220**,** 117049. doi: https://doi.org/10.1016/j.neuroimage.2020.117049.

Vinh, N.X., Epps, J., and Bailey, J. (2010). Information theoretic measures for clusterings comparison: Variants, properties, normalization and correction for chance. *The Journal of Machine Learning Research* 11**,** 2837-2854.

Vollenweider, F.X., Vollenweider-Scherpenhuyzen, M.F.I., Bäbler, A., Vogel, H., and Hell, D. (1998). Psilocybin induces schizophrenia-like psychosis in humans via a serotonin-2 agonist action. *NeuroReport* 9(17).

Wojtas, A., Bysiek, A., Wawrzczak-Bargiela, A., Szych, Z., Majcher-Maślanka, I., Herian, M., et al. 2022. Effect of Psilocybin and Ketamine on Brain Neurotransmitters, Glutamate Receptors, DNA and Rat Behavior. *International Journal of Molecular Sciences* [Online], 23(12).

Wyass, J.M., and Van Groen, T. (1992). Connections between the retrosplenial cortex and the hippocampal formation in the rat: A review. *Hippocampus* 2(1)**,** 1-11. doi: 10.1002/hipo.450020102.

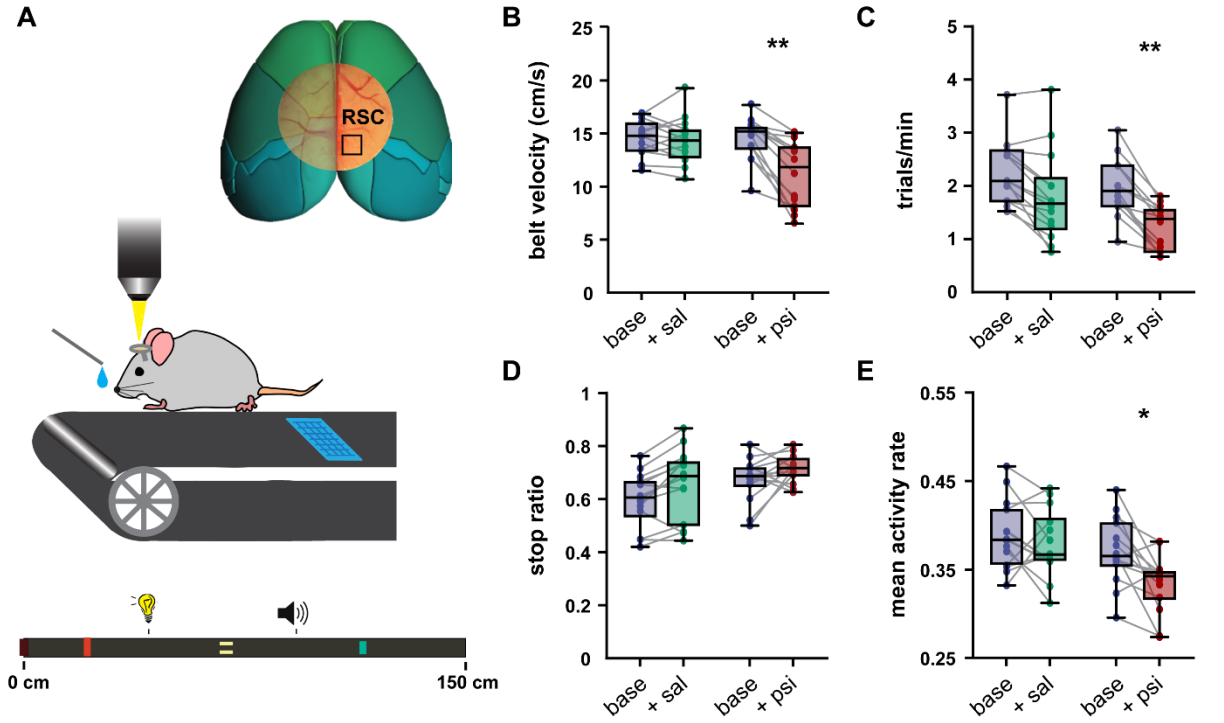

517

518 **Fig. 1. Behavioural effects of psilocybin.** A. Illustration of experimental setup and location of the
519 field of view over RSC (inset). Symbols on the treadmill belt indicate approximate locations of
520 tactile cues, as well as locations of visual and auditory cues. B. Box plots of the belt velocity
521 before/after saline/psilocybin administration. C. Number of trials per minute. D. Proportion of time
522 that mice were stationary during a trial. E. Mean activity rate of all neurons recorded simultaneously
523 in a session. Statistical significance ($p<0.05$) is indicated by '*', and ($p<0.01$) is indicated by '**'.
524 Dots are averages from each session.

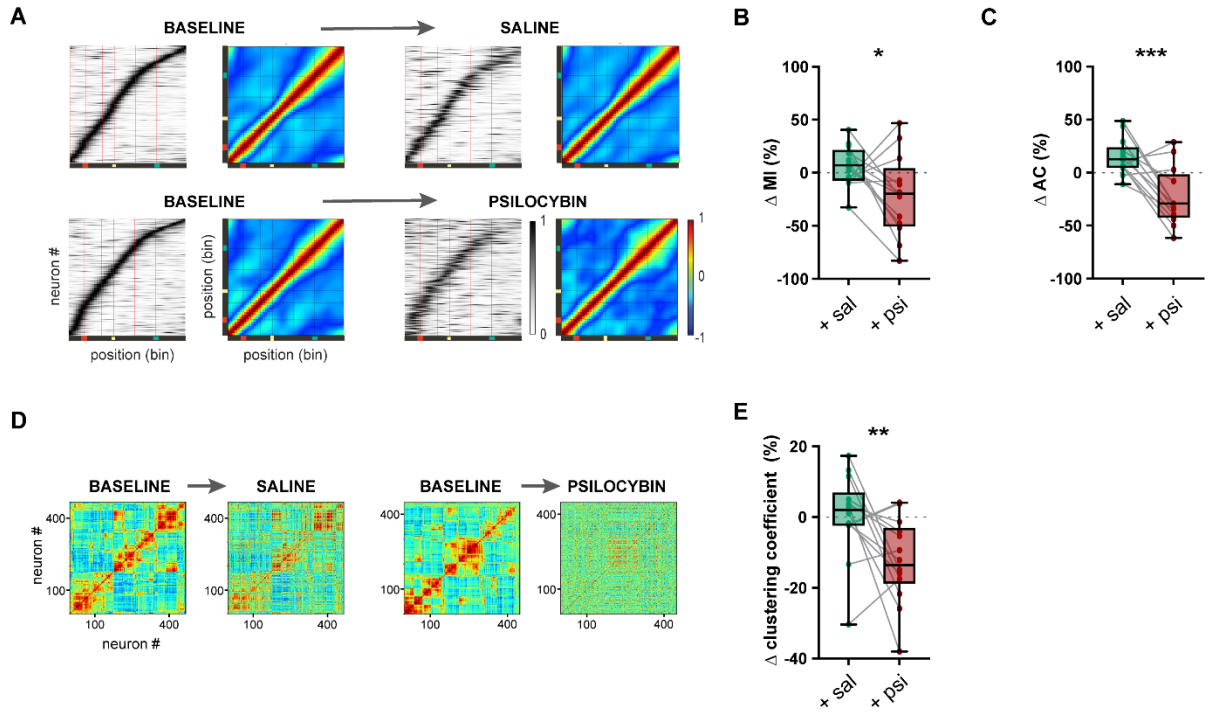

525

526 **Fig. 2. Effects of psilocybin on spatial encoding by neurons in the RSC.** A. Leftward panels
527 (black/white) show session-averaged activity of all position-tuned cells ordered by lag to peak
528 activity. The abscissa is treadmill belt position, the ordinate is individual neurons, and shade
529 indicates average normalized activity density of each neuron along the belt. Darker shade is higher
530 activity. Rightward panels (color) shows the mean autocorrelation of activity for the same cells.
531 Grouped panels show aggregated data from the same sessions before (left two panels) and after
532 (right two panels) injection. Sessions testing saline (top) were separate from those testing
533 psilocybin (bottom). The cue zones are indicated by red vertical lines. B. Box plots and individual
534 session-averaged values of percentage change of the mean mutual information (MI) with respect
535 to baseline within each recording session. C. Percentage change of the average trial-to-trial
536 correlation (AC) with respect to baseline within each recording day. D. Pairwise correlation
537 matrices of unit activity in one representative session before/after saline (top row) and before/after
538 psilocybin (bottom row). E. Percentage change of the means connectivity coefficients within each

recording session. Statistical significance ($p<0.05$) is indicated by '*', ($p<0.01$) is indicated by '**', and ($p<0.001$) is indicated by '***'.

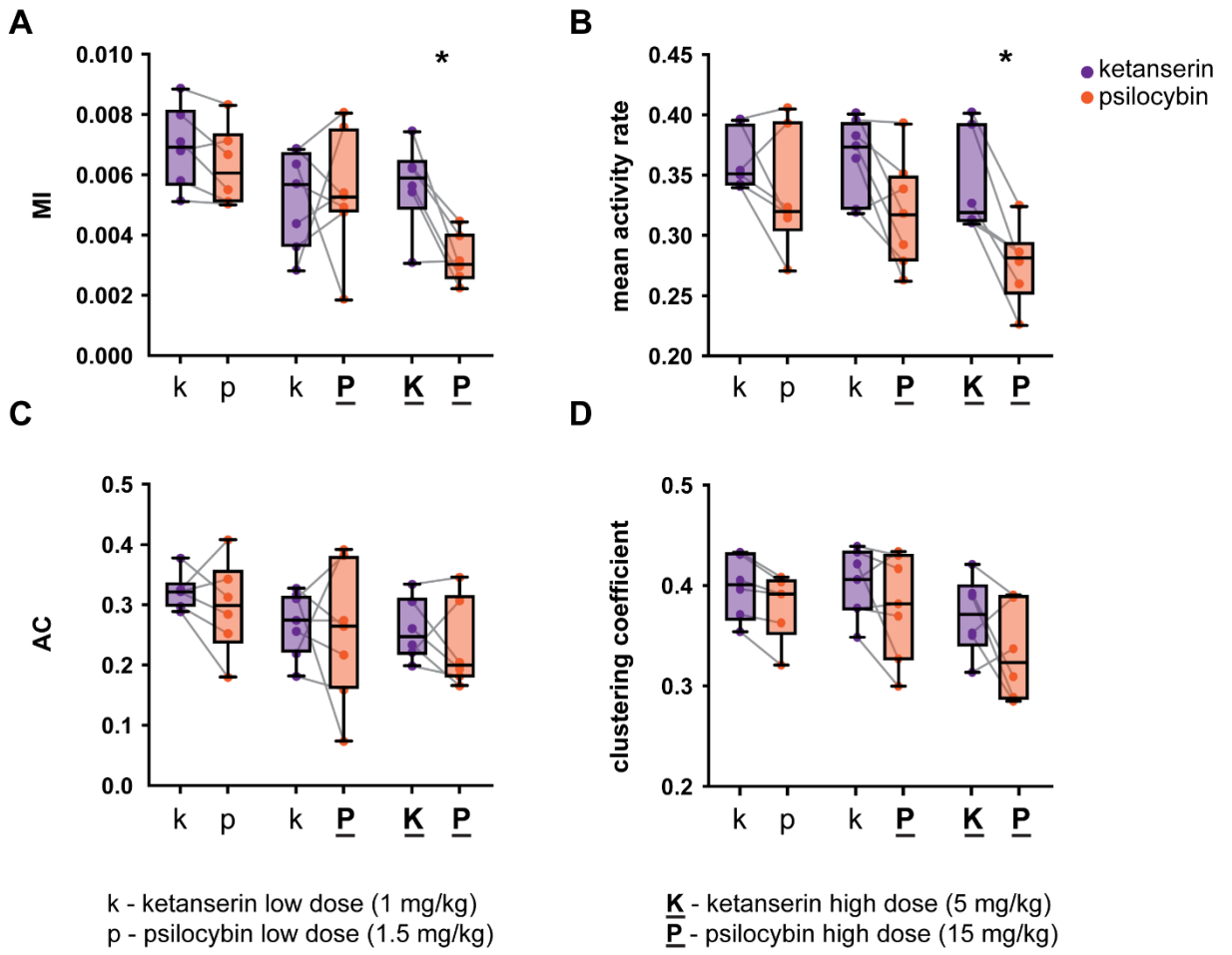

Fig. 3. Effects of ketanserin pretreatment on psilocybin-mediated changes in RSC spatial encoding. A. Box plots and individual values of adjusted mutual information (MI) for the different dose combinations with either low (k; 1 mg/kg) or high (**K**; 5 mg/kg) ketanserin pretreatment and low (p; 1.5 mg/kg) or high (**P**; 15 mg/kg) psilocybin administration. B. Box plots and individual values of average firing rates for each group. C. Mean trial-to-trial correlations (AC). D. Mean connectivity coefficients. Statistical significance ($p<0.05$) is indicated by '*'.

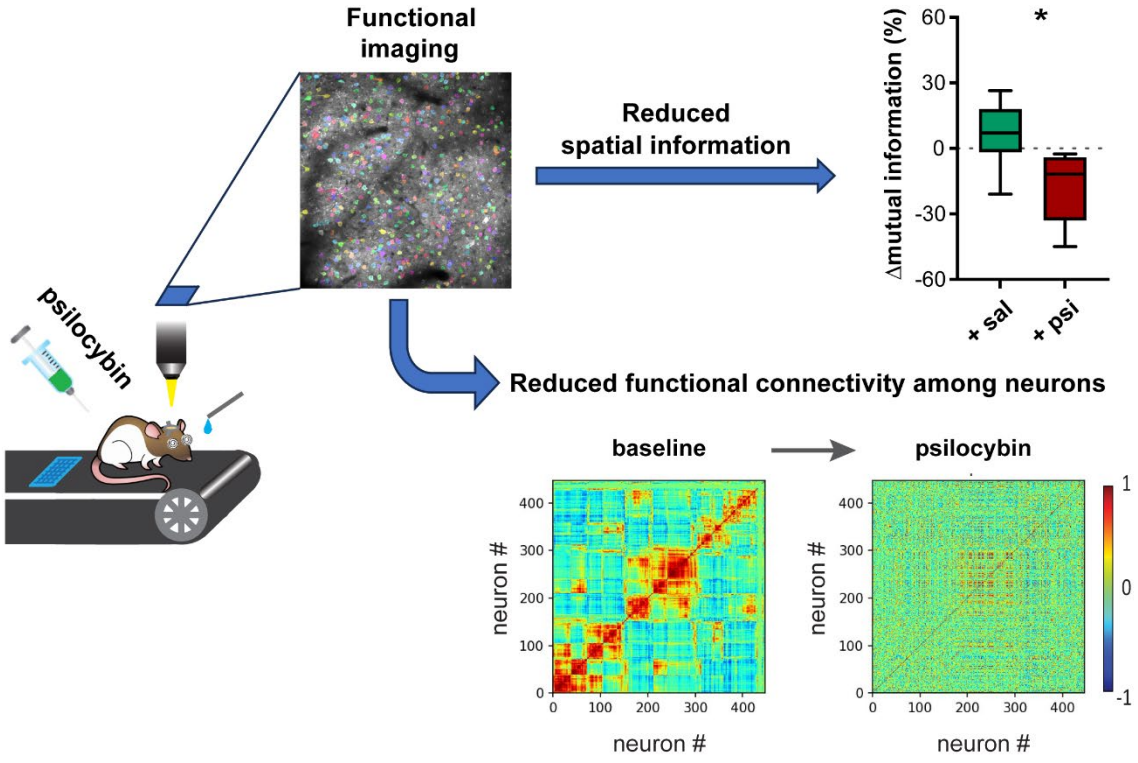

549

550

551 **Graphical abstract.** Administration of psilocybin in head-fixed mice navigating on a treadmill
552 decreases the place specificity and functional connectivity among simultaneously recorded
553 neurons in the retrosplenial cortex.